

Electronical Supporting Information

Sulfoxide-functionalized Nanogels inspired by the Skin Penetration Properties of DMSO

Doğuş Işık,¹ Aaroh Anand Joshi,¹ Xiao Guo,² Fiorenza Rancan,² André Klossek,³ Annika Vogt,² Eckart Rühl,³ Sarah Hedtrich,^{1,4} Daniel Klinger^{1}*

¹ Institute of Pharmacy, Freie Universität Berlin, Königin-Luise-Straße 2-4, 14195 Berlin, Germany

² Clinical Research Center of Hair and Skin Science, Department of Dermatology and Allergy, Charité – Universitätsmedizin Berlin, Charitéplatz 1, 10117 Berlin, Germany

³ Physical chemistry, Institute for Chemistry and Biochemistry, Freie Universität Berlin, Arnimallee 22, 14195 Berlin, Germany

⁴ The University of British Columbia, Faculty of Pharmaceutical Sciences, 2405 Wesbrook Mall, Vancouver, V6T1Z3, BC, Canada

** E-mail: daniel.klinger@fu-berlin.de*

Content

I. Monitoring the conversion of the Pre-NP network with functional amines	2
II. Investigation of functional groups in the nanogel network	3
III. Determination of incorporation efficiencies of functional amines	4
IV. Investigation of Swelling Behavior	6
V. Determination of Nile red loading and FITCA functionalization	8
VI. Supplement for stimulated Raman spectromicroscopy of the SC	10
VII. Materials and Syntheses	11

I. Monitoring the conversion of the Pre-NP network with functional amines

Quantitative conversion of the PFP ester groups was demonstrated for all functional nanogels by the disappearance of the PFP ester peaks in ^{19}F -NMR spectra (see Fig. S1).

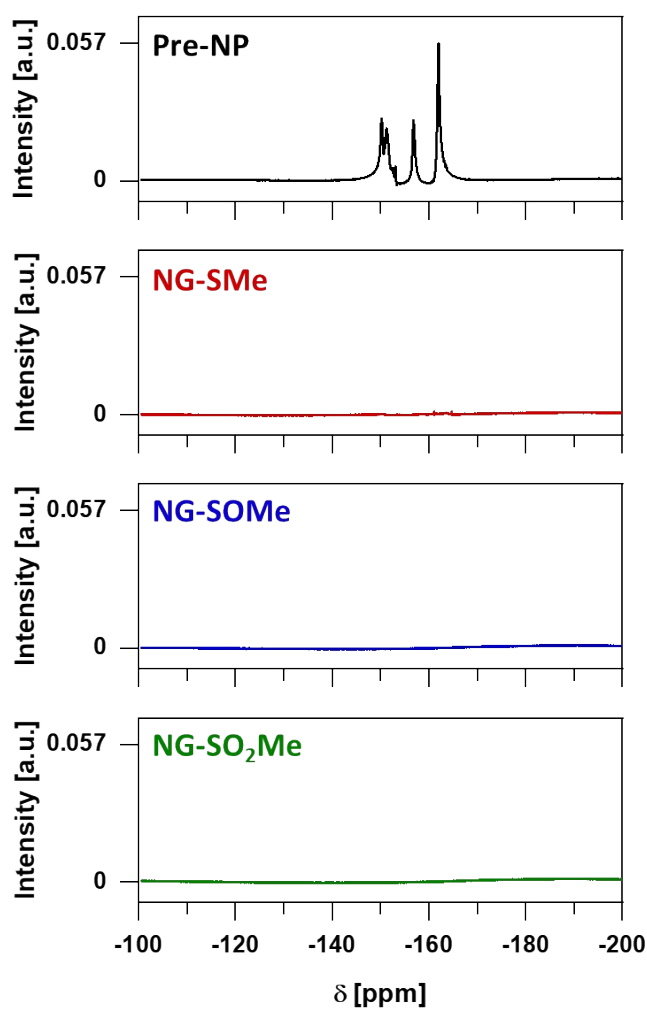


Fig. S1 Successful network functionalization is demonstrated by the disappearance of PFP ester peaks in ^{19}F -NMR spectra of all functional nanogels.

II. Investigation of functional groups in the nanogel network

Demonstrating control over the nanogel functionality also requires revealing the presence of the respective functional groups in the actual nanogel network. ATR-FTIR spectroscopy showed the presence of new signals, which can be assigned to the sulfoxide and sulfone moieties. In the NG-SO₂Me nanogels, the bands at 1291 and 1128 cm⁻¹ were ascribed to the sulfone groups. In the NG-SOMe nanogels, the peak at 994 cm⁻¹ is characteristic for sulfoxide moieties (see Fig. S2).

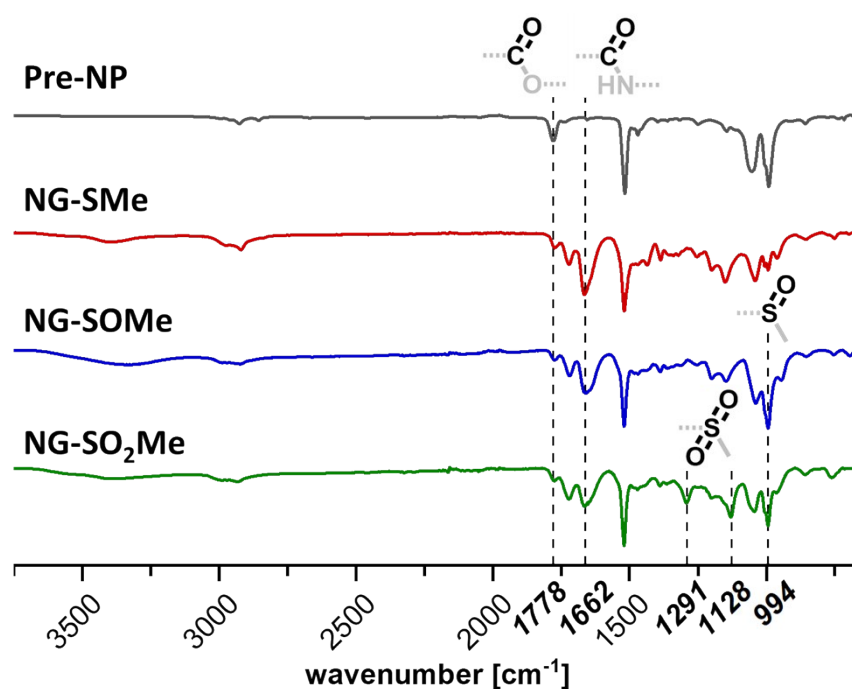


Fig. S2 Successful network functionalization was demonstrated by the disappearance of the reactive PFP ester bands of Pre-NPs and the simultaneous appearance of the functionalized amide bands for NG-SMe, NG-SOMe, and NG-SO₂Me nanogels as well as characteristic sulfoxide and sulfone bands for NG-SOMe and NG-SO₂Me in ATR-FTIR spectra, respectively.

III. Determination of incorporation efficiencies of functional amines

In order to determine the incorporation efficiencies of the different functional moieties into the reactive particle network, ^1H NMR spectroscopy was carried out. However, line broadening in the ^1H NMR spectra limits the determination accuracy for the cross-linked nanogels (Fig. S3 A, B). Thus, control experiments on linear polymer analogues were performed to gain further insights into the efficiency of the functionalization reaction. Post-modification reactions of reactive precursor polymers were carried out with all functional amines. As shown in Fig. S3 A, B the incorporation of all functional amine moieties could be verified through the respective peaks in the linear homopolymers and in the crosslinked polymer networks.

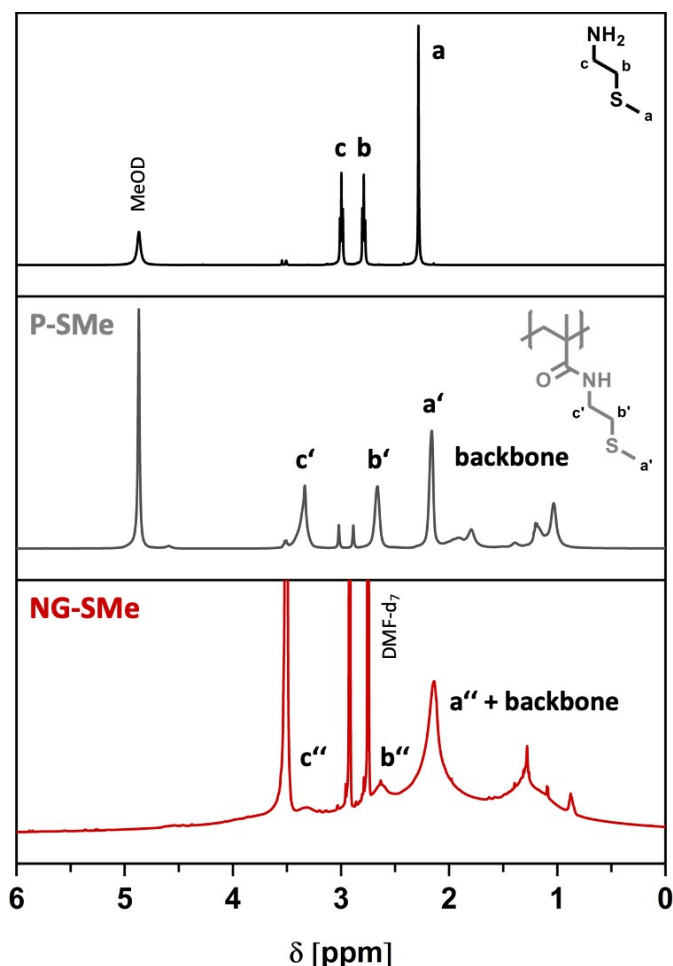


Fig. S3A Comparison between ^1H NMR spectra of the thioether functional amine, the homopolymer analogue and the corresponding functional nanogel. The P-SMe spectrum exhibits two weak DMF artefact signals at around 3 ppm.

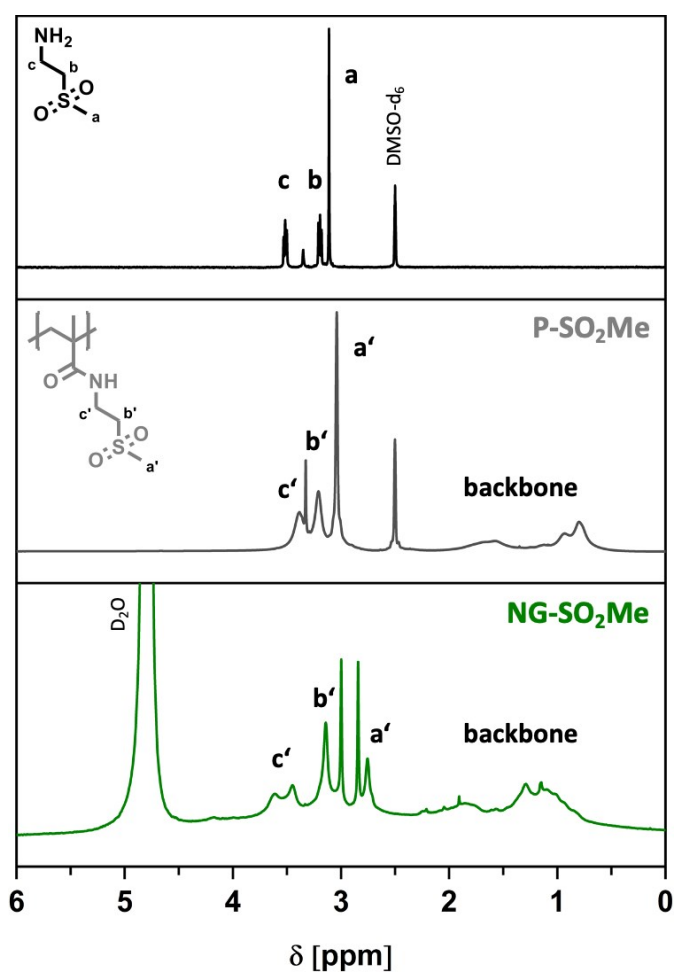


Fig. S3B Comparison between ^1H NMR spectra of the sulfone functional amine, the homopolymer analogue, and the corresponding functional nanogel. The NG-SO₂Me spectrum exhibits two DMF artefact signals at around 3 ppm.

IV. Investigation of Swelling Behavior

The sizes of the non-swollen functional nanogels were determined by evaluating TEM images of the respective dried nanoparticles. The diameter of 200 nanogels of each sample was determined with the software ImageJ (version 1.52e). The evaluation of TEM images showed similar sizes and size distributions for nanogels with different network amphiphilicity. These are similar in size to the reactive precursor particles (Fig. S4, left row). For the functional nanogels in aqueous medium, angle-dependent DLS measurements were conducted. These measurements showed that the sizes of the functionalized amphiphilic nanogels deviate significantly from the sizes of their respective Pre-NP (Fig. S4, right row). The observed discrepancy between swollen nanogels and precursor particles can be attributed to the difference in hydrophobic/hydrophilic nature of the introduced functional thioether, sulfoxide, and sulfone pending groups.

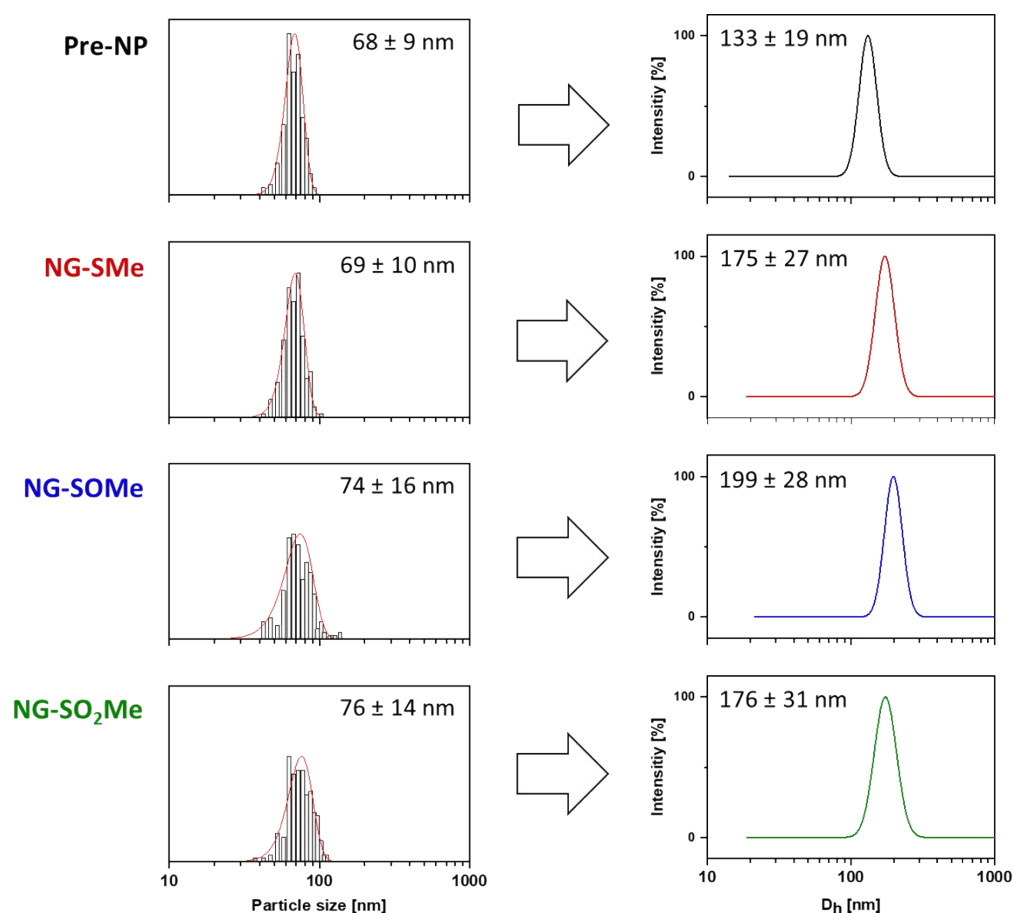


Fig. S4 Statistical evaluations of TEM images of all functional nanogel in dry state (left column). The red curves represent Gaussian fit functions. DLS curves were measured for the corresponding nanogels after dispersion in aqueous media (right row). The measurements were shown exemplary for an angle of 90°. Error limits are derived from the widths of the size distributions at full width at half maximum (FWHM).

In general, particle size distributions were determined by dynamic light scattering, performed on a Nicomp Nano Z3000 (Particle Sizing Systems, Port Richey, USA). The measurements were carried out at RT on aqueous dispersions. Angle-dependent measurements were carried out at scattering angles of 70°, 80°, 90°, 100°, and 110°, respectively. The apparent diffusion coefficient (D_{app}) of the Nicomp Nano Z3000 systems cumulant analysis of the autocorrelation function was used and plotted against the quadratic scattering vector (q^2). The z-average diffusion coefficient (D_s) was obtained from the y-intercept of the linear fit of the plotted data (Fig. S4.1) Finally, D_s was used to calculate the hydrodynamic diameter (D_h) of the nanogels.

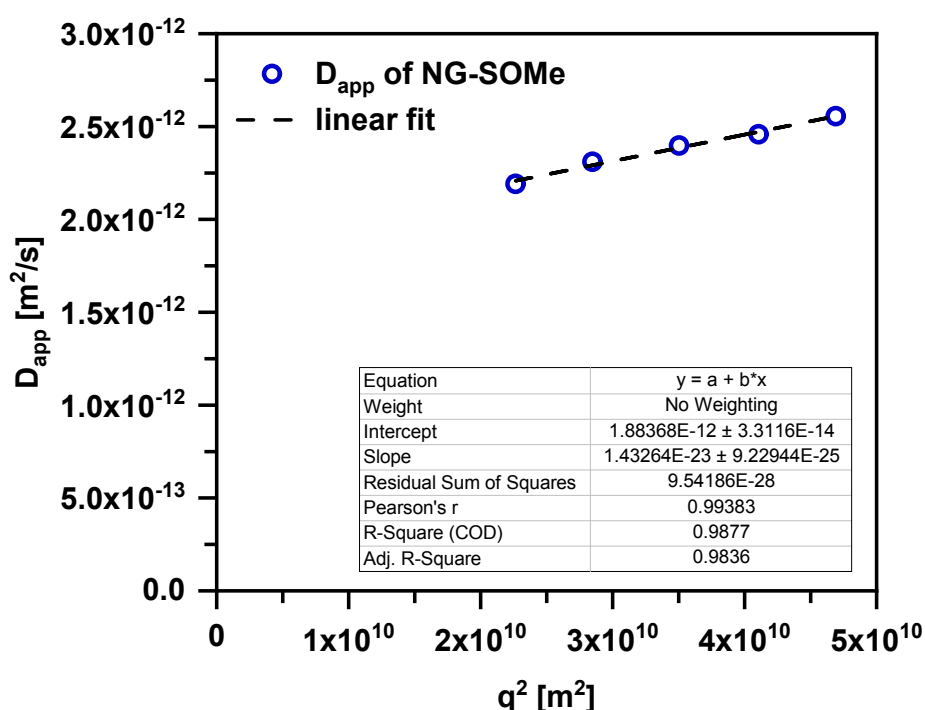


Fig. S4.1 The apparent diffusion coefficient (D_{app}) plotted against the quadratic scattering vector (q^2). Representative graph shown for NG-SOME nanogels.

V. Determination of Nile red loading and FITCA functionalization

To investigate the influence of the different network compositions on the topical delivery efficacy of the nanogels, Nile red (NR) was chosen as an uncharged, water-insoluble, and photostable model compound that strongly fluoresces bright red in hydrophobic environments. Therefore, all functional nanogels were loaded with NR via the co-solvent method. Aqueous dispersions of the respective nanogels were mixed with a solution of NR in acetone from which the organic solvent was evaporated subsequently, causing the diffusion of the hydrophobic dye into the nanogels. Encapsulated NR was determined by UV/Vis measurements on freeze-dried nanogels redispersed in DMSO. Quantification was achieved relative to a Nile red calibration curve (see ESI Fig. S5 (A)) confirming a loading capacity of 0.3 wt% for all functional nanogels (see ESI Fig. S5 (B)).

In addition, the penetration trajectory of the nanogels was traced by labeling all polymeric carriers with [2-(aminoethyl)-carbamoethyl]-5-aminofluorescein (FITCA). This was achieved by reacting a master batch of Pre-NPs with 3.65 wt% of FITCA ensuring the same incorporation of the fluorescent dye into the reactive nanogel network (see ESI Fig. S5 (B)). The follow-up reaction with the respective functional amines resulted than in the functional FITCA-labeled nanogels.

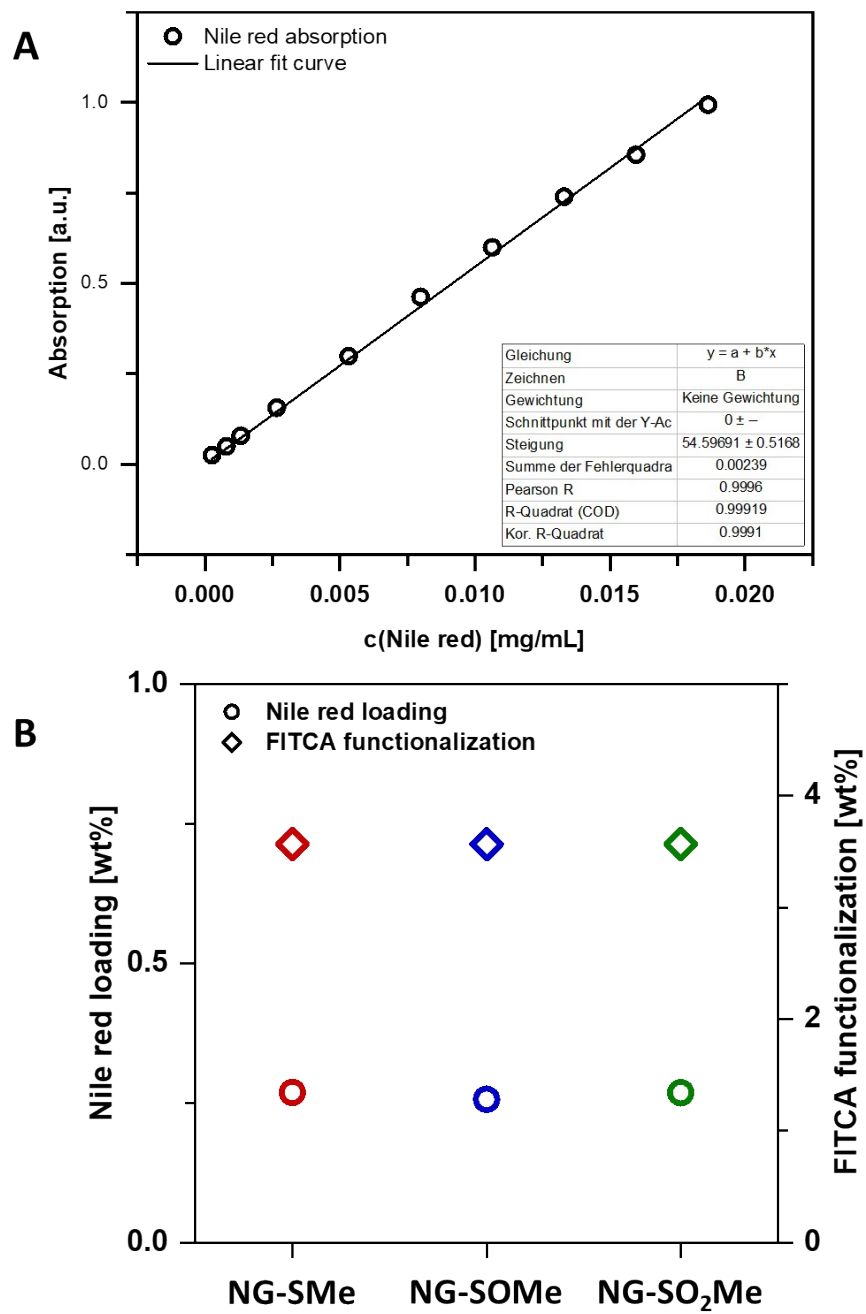


Fig. S5 Calibration curve of Nile red in DMSO at 552 nm (A) and determination of Nile red loading capacity and FITCA functionalization of all functional nanogels (B).

VI. Supplement for stimulated Raman spectromicroscopy of the SC

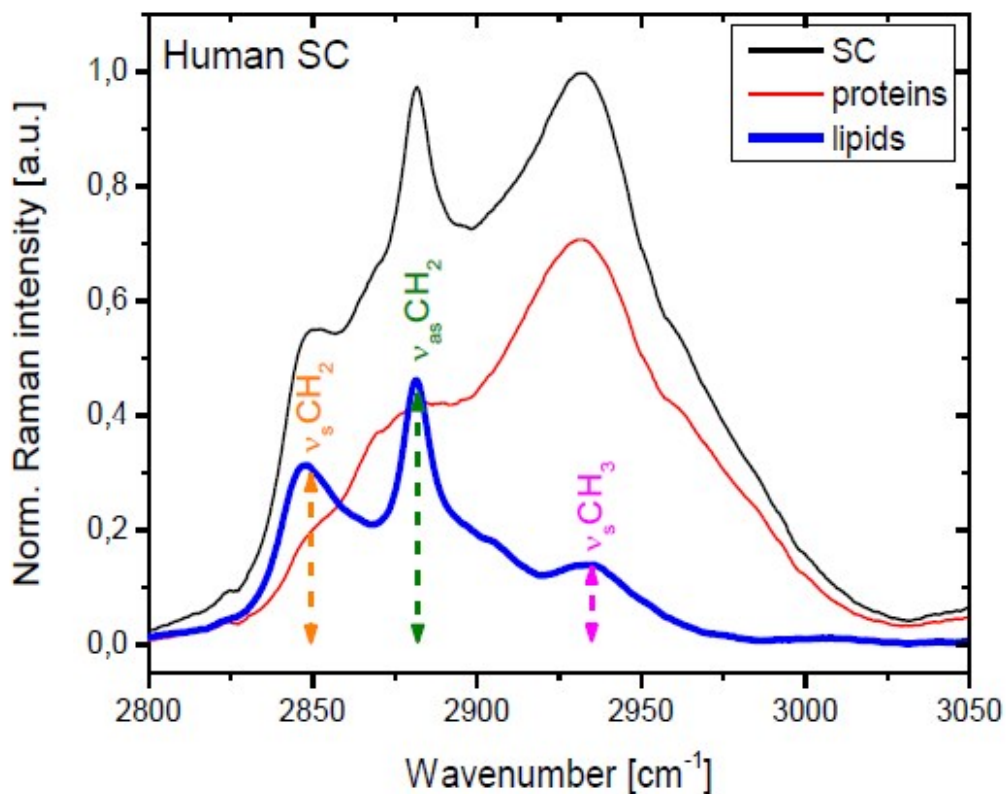


Fig. S6 Raman spectra of lipid-rich (blue) and protein-rich (red) regions in human skin (black) measured by stimulated Raman spectroscopy. The stretching vibrations $\nu_s(\text{CH}_2) = 2850 \text{ cm}^{-1}$ (lipids) and $\nu_s(\text{CH}_3) = 2934 \text{ cm}^{-1}$ (proteins) were conducted for the histological evaluation of the stratum corneum.

VII. Materials and Syntheses

Materials

All starting materials and reagents were purchased from commercial sources and used without further purification, unless otherwise stated. Methacryloyl chloride (97%), pentafluorophenol (99%), triethylamine (TEA) (99%) and fluorescein isothiocyanate isomer 1 (95%) were purchased from *abcr GmbH*. 2,6-lutidine (99+%) and *n*-hexadecane (99%) were purchased from *Alfa Aesar*. Sodium dodecyl sulfate (SDS), ethylene glycol dimethacrylate (EGDMA) (>97,5%) and ethylenediamine were purchased from *Merck KGaA*. Sodium methoxide solution (25 wt% in methanol), 2,2'-azobis(2-methylpropionitrile) (AIBN) (98%) and 2,6-di-*tert*-butyl-*p*-cresol (>99%) were purchased from *Sigma-Aldrich*. 2-(Methylthio)ethylamine (MTEA) (95%) and Nile red were purchased from *Fluorochem Ltd*. Hydrogen peroxide (30%) was purchased from *Carl Roth GmbH*. Anhydrous solvents were taken from a MBraun MB-SPS-800 solvent purification system. Ultrapure water was taken from a LaboStar UV 2 water system. MAES,^[1] FITCA,^[2] PFPMA,^[3, 4] pPFPMA^[4] and Pre-NP^[5] were synthesized according to literature procedures. Moisture and/or air sensitive reactions were carried out in dry glassware under nitrogen atmosphere. Dialyses were performed in benzoylated cellulose dialysis tubes purchased from Sigma-Aldrich (width: 32 mm, MWCO 2000 g mol⁻¹).

Syntheses

Synthesis of 2-aminoethyl methyl sulfoxide (AEMS)^[1] Briefly, 2-methylsulfanyl ethylamine (1.00 g, 11 mmol, 1.0 eq.) was dissolved in 5 mL DI water and the solution was adjusted to pH 5 with the use of 37% HCl. 1.1 mL of 30% H₂O₂ (11 mmol, 1 eq.) was added dropwise to the reaction mixture while stirring at 0 °C. The mixture was allowed to warm to RT while stirring overnight. Subsequently, the solvent was evaporated, the resulting oily residue was dissolved in 25 mL MeOH and the solution was adjusted to pH 9.5 by using 25 wt% sodium methoxide in MeOH. After filtration and evaporation of the solvent 1.13 g (11.5 mmol, 96%) of a colorless oily liquid was obtained without further purification. ¹H NMR (500 MHz, CD₃OD): δ = 3.27 (m, 2H, H₂N-CH₂), 3.11 (m, 1H, CH₂-S), 2.96 (m, 1H, CH₂-S), 2.69 (s, 3H, CH₃) ppm; ¹³C NMR (151 MHz, D₂O): δ = 54.89, 36.79, 34.60; IR (ATR-FTIR): $\tilde{\nu}$ = 3280 (br), 2910 (m), 2824

(m), 1610 (w), 1461 (w), 1408 (m), 1305 (w), 1015 (s), 946 (s), 826 (w), 770 (w), 695 (m) cm^{-1} . HRMS: calc. for $\text{C}_3\text{H}_9\text{NOS}$ $[\text{M} + \text{H}]^+$: 108.0478, found $[\text{M} + \text{H}]^+$: 108.0479.

Synthesis of [2-(aminoethyl)-carbamothioyl]-5-aminofluorescein (FITCA)^[2] A solution of fluorescein isothiocyanate isomer 1 (0.1 g, 0.26 mmol, 1 eq.) in 10 mL MeOH was added dropwise to a solution of ethylenediamine (17.2 μL , 0.26 mmol, 1 eq.) in 10 mL MeOH. The reaction mixture was stirred overnight at RT. The solvent was evaporated and the crude product was freeze-dried from DI water to yield 113 mg (98%) of a bright orange powder. ^1H NMR (500 MHz, $\text{DMSO-}d_6$): δ = 8.31 (s, 1H, Ar^1), 7.79 (d, J = 8.5, 1H, Ar^1), 7.18 (d, J = 8.4 Hz, 1H, Ar^1), 6.73-6.65 (m, 2H, $\text{Ar}^{2,3}$), 6.64 – 6.50 (m, 4H, $\text{Ar}^{2,3}$), 3.71 (s, 2H, SCNH-CH_2), 2.98 (t, J = 6.4 Hz, 2H, $\text{CH}_2\text{-NH}_2$), 2.78 (s, 2H, NH_2) ppm. HRMS: calc. for $\text{C}_{23}\text{H}_{19}\text{N}_3\text{O}_5\text{S}$ $[\text{M} + \text{H}]^+$: 450.1124, found $[\text{M} + \text{H}]^+$: 450.1122.

Synthesis of pentafluorophenyl methacrylate (PFPMA)^[3, 4] Pentafluorophenol (16.2 g, 88.0 mmol, 1.0 eq.) and 2,6-lutidine (10.5 mL, 90.2 mmol, 1.0 eq.) were dissolved in 150 mL dry DCM under ice cooling, 8.7 mL methacryloyl chloride (89.1 mmol, 1.0 eq.) was added dropwise to the reaction mixture which was then allowed to reach RT while stirring overnight. The precipitate was filtered off and the filtrate was washed three times with 100 mL DI water and once with sat. NH_4Cl before drying over MgSO_4 . A spatula tip of 2,6-di-*tert*-butyl-*p*-cresol was added to the solution as polymerization inhibitor. After the solvent was removed the crude oily product was distilled under reduced pressure (0.02 mbar, 26 – 27 $^\circ\text{C}$) to yield 13.53 g (53.66 mmol, 61 %) of a colorless liquid. ^1H NMR (500 MHz, CDCl_3): δ = 6.45 (s, 1H, H_{cis}), 5.90 (s, 1H, H_{trans}), 2.09 (s, 3H, CH_3) ppm; ^{19}F NMR (376 MHz, CDCl_3): δ = -152.83 (d, J = 20.8 Hz, 2F, F_{ortho}), -158.26 (t, J = 21.9 Hz, 1F, F_{para}), -162.54 (t, J = 20.5 Hz, 2F, F_{meta}) ppm.

Synthesis of reactive poly(pentafluorophenyl methacrylate) precursor nanoparticles (Pre-NP)^[5] *Aqueous phase*: SDS was dissolved in DI water (100 mL, 1.25 mg/mL, 2.5 wt% w.r.t PFPMA). *Dispersed phase*: PFPMA (5.0 g, 19.8 mmol) was mixed with EGDMA (0.2 g, 1.00 mmol, 5 mol% w.r.t PFPMA) filtered previously over basic aluminum oxide, *n*-hexadecane (0.22 g, 0.97 mmol) and AIBN (100 mg, 0.6 mmol). Both phases were combined and pre-sonicated in a sonication bath for 5 minutes. Full dispersion was achieved by ultrasonication with a Branson Sonifier SFX 550 (pulse duration: 15 seconds, pause duration: 15 seconds, total pulse duration: 4

minutes). The miniemulsion was purged with nitrogen for 10 minutes and the polymerization was performed overnight at 75 °C while stirring. The size of the particles (as synthesized) were determined by dynamic light scattering of diluted dispersions. Subsequently, the dispersion was centrifuged for 30 minutes at 9900 RPM after which the supernatant was removed and replaced with DI water. The particles were dispersed again by vortexing and sonication. This washing procedure was repeated 5 times and the particles were freeze-dried from DI water to give a white powder in an average yield of 66%. ATR-FTIR spectroscopy was used to investigate potential hydrolysis of the particles in their solid state.

Synthesis of 4-Cyano-4-(phenylcarbonothioylthio)pentanoic acid (CPCTPA)^[6]

Carbon disulfide (0.86 mL, 14.2 mmol, 1.8 eq.) was added dropwise to an anhydrous solution of phenyl magnesium bromide (7.8 mL, 7.8 mmol, 1 M solution in THF, 1 eq.) in 2.2 mL THF until the solution slightly boiled. After stirring for 1 hour at RT the reaction mixture was added to 50 g of ice and acidified with 37 wt% HCl. The deep purple solution was then extracted with diethyl ether twice and dried in *vacuo* to yield a deep purple oil. The crude dithiobenzoic acid was used directly without further purification and added to ACVA (2.2 g, 7.8 mmol, 1 eq.) in 20 mL ethyl acetate. The suspension was degassed by three consecutive freeze-pump-thaw cycles and refluxed under nitrogen atmosphere overnight. The solvent was then removed in *vacuo* and the crude product was purified twice by column chromatography (*n*-hexane/ethyl acetate 1:2.5) to yield 830 mg (3 mmol, 38 %) of a red solid. ¹H NMR (500 MHz, CDCl₃): δ = 7.91 (d, J = 7.4 Hz, 2H, *o*-Ar-H), 7.57 (t, J = 7.3 Hz, 1H, *p*-Ar-H), 7.40 (t, J = 7.7 Hz, 2H, *m*-Ar-H), 2.83 – 2.39 (m, 4H, CH₂-CH₂), 1.94 (s, 3H, CH₃) ppm; ¹³C NMR (126 MHz, CDCl₃): δ = 222.31, 177.07, 144.64, 133.22, 128.74, 126.83, 118.52, 45.75, 33.17, 29.64, 24.32 ppm.

Synthesis of linear reactive poly(pentafluorophenyl methacrylate) (pPFPMA)^[4, 7]

Briefly, PFPMA (3.00 g, 11.9 mmol, 1.0 eq.), CPCTPA (22.2 mg, 79.3 μmol, 0.0067 eq.) and AIBN (1.63 mg, 9.91 μmol, 0.00084 eq.) were dissolved in 5.95 mL dry THF in a predried schlenk flask under nitrogen atmosphere. The reaction mixture was purged with nitrogen for 30 minutes and the polymerization was performed overnight at 75 °C while stirring. The crude product was purified by precipitating twice in cold MeOH and drying in *vacuo* to yield 1.73 g (6.86 mmol, 58%) of a pinkish powder. ¹H NMR (500 MHz, CDCl₃): δ = 2.65 – 2.03 (m, 2H, -CH₂), 1.64 – 1.24 (m, 3H, -CH₃) ppm;

^{19}F NMR(376 MHz, CDCl_3): $\delta = -150.64$ (d, $J = 76.0$ Hz, 1F, F_{ortho}), -151.67 (s, 1F, F_{ortho}), -157.13 (s, 1F, F_{para}), -162.30 (s, 2F, F_{meta}) ppm; GPC (DMF, 10 mmol LiBr, PS Standard) $M_n = 18300$ g mol $^{-1}$, PDI = 1.24; IR(ATR-FTIR): $\tilde{\nu} = 1777$ (m, C=O), 1516 (s), 1470 (m), 1267 (w), 1144 (w), 1052 (s), 991 (s), 857 (w), 733 (w) cm $^{-1}$.

Synthesis of functional thioether, sulfoxide and sulfone polymers (P-SMe, P-SOMe, P-SO₂Me) The post-polymerization modification of pPFPMA was performed according to a procedure reported by Gibson et al.^[8] Briefly, pPFPMA (1.50 g, 5.95 mmol, 1.0 eq.) was dissolved in 90 mL DMF. The solution was divided into three equal parts (30 mL each) and to each part a different amino-functionalized sulfur moiety was added with each time TEA (830 μL , 5.94 mmol, 3.0 eq. w.r.t. PFPMA monomer units): For P-SMe: MTEA (542 mg, 5.94 mmol, 3.0 eq. w.r.t. PFPMA monomer units), for P-SOMe: AEMS (638 mg, 5.95 mmol, 3.0 eq. w.r.t. PFPMA monomer units), and for P-SO₂Me: MSEA (723 mg, 5.86 mmol, 3.0 eq. w.r.t. PFPMA monomer units). The reaction mixtures were then heated to 50 °C and stirred overnight. The functional polymers were then purified by extensive dialysis against DMF, DI water and finally ultrapure water to give yellowish powders after subsequent freeze-drying. P-SMe; ^1H NMR (600 MHz, $\text{DMSO-}d_6$); $\delta = 3.16$ (s, 2H, NH-CH₂), 2.50 (s, 2H, CH₂-S overlapping with $\text{DMSO-}d_6$), 2.06 (s, 3H, S-CH₃), 1.91 – 1.39 (m, 2H, CH₂), 1.29 – 0.74 (m, 3H, CH₃) ppm; P-SOMe; ^1H NMR (600 MHz, $\text{DMSO-}d_6$); $\delta = 3.31$ (s, 2H, NH-CH₂ overlapping with traces of H₂O), 2.91 (s, 1H, CH₂-SO), 2.77 (s, 1H, CH₂-SO), 2.58 (s, 3H, SO-CH₃), 2.19 – 1.46 (m, 2H, CH₂), 1.36 – 0.73 (m, 3H, CH₃) ppm; P-SO₂Me; ^1H NMR (600 MHz, $\text{DMSO-}d_6$); $\delta = 3.33$ (s, 2H, NH-CH₂ overlapping with CH₂-SO₂), 3.23 (s, 2H, CH₂-SO₂ overlapping NH-CH₂), 3.03 (s, 3H, SO₂-CH₃), 2.23 – 1.52 (m, 2H, CH₂), 1.44 – 0.80 (m, 3H, CH₃) ppm.

References

- [1] J. Lydon, E. Deutsch, *Inorg. Chem.* **1982**, *21*, 3180-3185.
- [2] R. Gentsch, F. Pippig, K. Nilles, P. Theato, R. Kikkeri, M. Maglinao, B. Lepenies, P. H. Seeberger, H. G. Börner, *Macromolecules* **2010**, *43*, 9239-9247.
- [3] J.-C. Blazejewski, J. W. Hofstraat, C. Lequesne, C. Wakselman, U. E. Wiersum, *J. Fluorine Chem.* **1998**, *91*, 175-177.
- [4] M. Eberhardt, R. Mruk, R. Zentel, P. Théato, *Eur. Polym. J.* **2005**, *41*, 1569-1575.

- [5] A. Gruber, D. Işık, B. B. Fontanezi, C. Böttcher, M. Schäfer-Korting, D. Klinger, *Polym. Chem.* **2018**, *9*, 5572-5584.
- [6] S. H. Thang, Y. K. Chong, R. T. A. Mayadunne, G. Moad, E. Rizzardo, *Tetrahedron Lett.* **1999**, *40*, 2435-2438.
- [7] M. Eberhardt, P. Théato, *Macromol. Rapid Commun.* **2005**, *26*, 1488-1493.
- [8] M. I. Gibson, E. Fröhlich, H. A. Klok, *J. Polym. Sci., Part A: Polym. Chem.* **2009**, *47*, 4332-4345.